Lanthanide Nano-Bioprobes

DOI: 10.1002/ange.201405937

Dissolution-Enhanced Luminescent Bioassay Based on Inorganic Lanthanide Nanoparticles**

Shanyong Zhou, Wei Zheng, Zhuo Chen, Datao Tu, Yongsheng Liu, En Ma, Renfu Li, Haomiao Zhu, Mingdong Huang, and Xueyuan Chen**

Abstract: *Conventional dissociation-enhanced lanthanide fluoroimmunoassays (DELFIA) using molecular probes suffer from a low labeling ratio of lanthanide ions (Ln^{3+}) per biomolecule. Herein, we develop a unique bioassay based on the dissolution-enhanced luminescence of inorganic lanthanide nanoparticles (NPs). As a result of the highly concentrated Ln^{3+} ions in a single Ln^{3+} NP, an extremely high Ln^{3+} labeling ratio can be achieved, which amplifies significantly the luminescence signal and thus improves the detection sensitivity compared to DELFIA. Utilizing sub-10 nm $NaEuF_4$ NPs as dissolution-enhanced luminescent nanoprobes, we demonstrate the successful in vitro detection of carcinoembryonic antigen (CEA, an important tumor marker) in human serum samples with a record-low detection limit of 0.1 pg mL^{-1} (0.5 fM). This value is an improvement of approximately 3 orders of magnitude relative to that of DELFIA. The dissolution-enhanced luminescent bioassay shows great promise in versatile bioapplications, such as ultrasensitive and multiplexed in vitro detection of disease markers in clinical diagnosis.*

Sensitive and specific biodetection is essential for a variety of biomedical applications, including protein identification, DNA immunoassays, and in early-stage cancer theranostics.[1] For in vitro biodetection, a low detection limit is a goal of general concern and is particularly critical for non-invasive analysis of human glandular secretions such as saliva.[2] Among diverse in vitro biodetection methods, luminescent bioassays are currently the primary analytical tool because of their convenient optical signal transduction, high sensitivity, and fast response.[3] Particularly, dissociation-enhanced lanthanide fluoroimmunoassay (DELFIA), as one of the most sensitive luminescent bioassay techniques, has been widely adopted in a variety of research and medical institutions.[4] DELFIA combines the advantages of a background-free signal from the time-resolved (TR) technique and the "antenna effect" of the luminescence enhancement solution. The technique is an excellent method to eliminate the interference of scattered light and other short-lived autofluorescence from biological samples or assay plates, thus offering remarkably high sensitivity relative to that of conventional fluorescence immunoassays (Figure S1, Supporting Information).[5] In a typical DELFIA (Figure 1a), a non-luminescent lanthanide (Ln^{3+}) chelate is employed as the molecular probe to label the analyte, which subsequently reacts with a weakly acidic enhancer solution and is transformed into a highly luminescent Ln^{3+} micelle.[4b] Unfortunately, molecular probes, such as Ln^{3+} chelates, often suffer from a low labeling ratio (up to 10–30 Ln^{3+} labels per biomolecule), thus providing limited TR photoluminescence (PL) signal and sensitivity in DELFIA.[6] Moreover, serious concerns over the chemical stability and high cost of Ln^{3+}-chelating agents may limit their practical application.

Inorganic lanthanide nanoparticles (NPs), emerging as a new class of TRPL nanoprobes and as an alternative to conventional molecular probes, have recently attracted

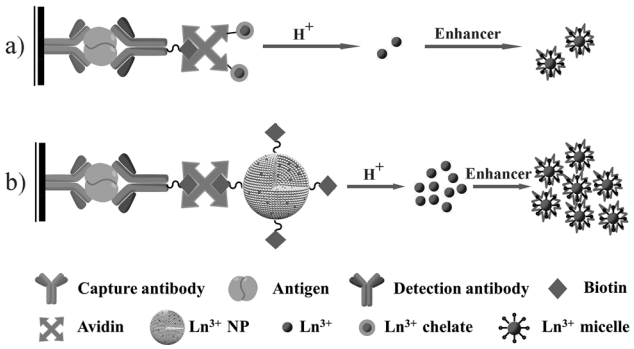

Figure 1. Schematic representation of a) conventional DELFIA immunoassay based on Ln^{3+} chelates and b) the proposed dissolution-enhanced luminescent bioassay (DELBA) based on inorganic Ln^{3+} NPs.

[*] S. Y. Zhou, Dr. W. Zheng, Dr. D. T. Tu, Dr. Y. S. Liu, E. Ma, R. F. Li, Dr. H. M. Zhu, Prof. X. Y. Chen
Key Laboratory of Optoelectronic Materials Chemistry and Physics and Key Laboratory of Design and Assembly of Functional Nanostructures, Fujian Institute of Research on the Structure of Matter
Chinese Academy of Sciences, Fuzhou, Fujian 350002 (China)
E-mail: xchen@fjirsm.ac.cn

S. Y. Zhou, Dr. Z. Chen, Prof. M. D. Huang, Prof. X. Y. Chen
State Key Laboratory of Structural Chemistry and
Danish-Chinese Centre for Proteases and Cancer
Fujian Institute of Research on the Structure of Matter
Chinese Academy of Sciences, Fuzhou, Fujian 350002 (China)
E-mail: mhuang@fjirsm.ac.cn

[**] We thank Prof. Weiping Su for helpful discussions and Dr. Xianren Ye in Fujian Provincial Cancer Hospital for kindly providing us with the human serum samples. This work is supported by the 973 program of MOST (No. 2014CB845605), Special Project of National Major Scientific Equipment Development of China (No. 2012YQ120060), the NSFC (Nos. 11204302, 11304314, U1305244, and 21325104), the Key Project of Science and Technology Foundation of Fujian Province (No. 2013H0060), the CAS/SAFEA International Partnership Program for Creative Research Teams, and Strategic Priority Research Program of the CAS (No. XDA09030307).

Supporting information (Experimental details) for this article is available on the WWW under http://dx.doi.org/10.1002/anie.201405937.

tremendous interest for their potential bioapplications.[7] Compared to Ln^{3+} chelates, inorganic Ln^{3+} NPs show many advantages, such as higher resistance to photobleaching, lower toxicity, greater flexibility for bioconjugation, and significantly lower cost.[8] However, owing to the parity-forbidden intra-4f^6 transitions within Ln^{3+} ions, their absorption is usually too low to yield intense PL, which results in low sensitivity in bioassays. To overcome this concern, the technique of lanthanide nanoprobes can be hybridized with the DELFIA procedure by simply replacing Ln^{3+} chelates with Ln^{3+} NPs in the labeling process. As illustrated in Figure 1b, as a result of the highly concentrated Ln^{3+} ions in a single NP, numerous Ln^{3+} ions are released and transformed into highly luminescent Ln^{3+} micelles after the dissolution of the NPs by the enhancer solution in the assay procedure. This process significantly amplifies the TRPL signal and thus improves the detection sensitivity compared to that of DELFIA.

Herein, we propose a unique bioassay method based on the dissolution-enhanced luminescence of inorganic Ln^{3+} NPs. To exemplify this concept, we have employed $NaEuF_4$ NPs as nanoprobes and 2-naphthoyltrifluoroacetone (β-NTA) as the enhancer solution in view of its high chelating and sensitizing ability with Eu^{3+} ions. We investigate the dissolution-enhanced PL of sub-10 nm $NaEuF_4$ NPs using high-resolution optical spectroscopy and dialysis experiments. Using the intense dissolution-enhanced PL of biotinylated $NaEuF_4$ NPs in a typical heterogeneous sandwich bioassay, we demonstrate the ultrasensitive and accurate detection of carcinoembryonic antigen (CEA) in human serum samples. Furthermore, we reveal that the proposed dissolution-enhanced luminescent bioassay (DELBA) can be extended to other Ln^{3+} NPs.

Monodisperse $NaEuF_4$ NPs were synthesized by a modified coprecipitation route.[9] The as-synthesized NPs were hydrophobic and can be readily dispersed in a variety of nonpolar organic solvents (Figure 2a). The TEM image of the NPs shows that the as-synthesized $NaEuF_4$ NPs were approximately spherical with an average diameter of 8.6 ± 0.5 nm (Figures 2b,d). The corresponding high-resolution TEM (HRTEM) image displays clear lattice fringes with a d spacing of 0.297 nm (Figure 2c), which is in good agreement with the lattice spacing of the (101) plane of hexagonal-phase $NaEuF_4$. The X-ray diffraction (XRD) pattern shows that all the diffraction peaks can be well indexed in accordance with hexagonal-phase $NaEuF_4$ (Figure 2e), thus confirming the formation of highly crystalline $NaEuF_4$ NPs. Compositional analysis by energy-dispersive X-ray spectroscopy revealed the presence of Na, Eu, and F elements in the NPs (Figure S2). Based on the NP size and the cell parameters of the $NaEuF_4$ crystals, the number of Eu^{3+} ions per NP was estimated to be 4334 ± 700.

To render the hydrophobic NPs hydrophilic and biocompatible, we removed the oleate ligands from their surface by acid treatment.[10] The successful removal of surface ligands was confirmed by FTIR spectra and thermogravimetric analysis (TGA) for NPs before and after acid treatment (Figures S3 and S4). As a result, these ligand-free NPs exhibited much better water solubility and can be readily dispersed in distilled water. Such acid treatment had no noticeable influence on the size and morphology of the NPs (Figure 3a and Figure S5). Moreover, as a result of the removal of surface ligands, positively charged Eu^{3+} ions were exposed on the surface of the ligand-free NPs, with the result that their colloidal solution had a positive ζ potential of $+48.6$ mV at pH 6.9 (Figure S6). As such, these ligand-free NPs can undergo direct conjugation with electronegative groups of biomolecules for further bioapplications.[10,11]

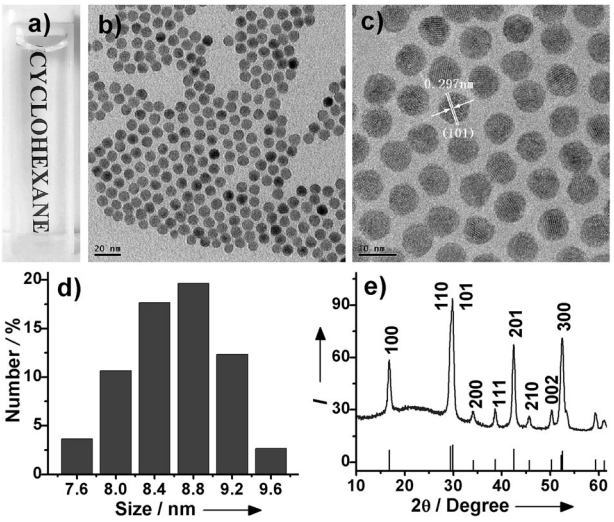

Figure 2. a) Photograph showing the transparency of the as-synthesized $NaEuF_4$ NPs dispersed in cyclohexane. b) TEM image (scale bar = 20 nm) and c) HRTEM image (scale bar = 10 nm) of $NaEuF_4$ NPs. d) Size distribution of $NaEuF_4$ NPs as obtained from 200 particles in the TEM image. e) Powder XRD pattern of $NaEuF_4$ NPs. The vertical lines represent the standard pattern of hexagonal-phase $NaEuF_4$ (JCPDS No. 049-1897).

To investigate the dissolution-enhanced PL behavior of Ln^{3+}-based NPs, we first dissolved ligand-free $NaEuF_4$ NPs in the enhancer solution (pH 2.3), consisting of Triton X-100, β-NTA, and tri-n-octylphosphine oxide (TOPO), where β-NTA has a very high affinity for Eu^{3+} ions ($\log k = 8.8$).[12] The TEM image shows the formation of a large quantity of smaller NPs within 1 minute upon addition of ligand-free NPs to the enhancer solution (Figure 3b), indicating that the original NPs undergo chemical dissolution. The dissolved NPs in the enhancer solution (1 μg mL^{-1}) displayed bright-red PL under UV lamp illumination at $\lambda = 300$ nm (Figure 3c), in sharp contrast to the NPs (1 mg mL^{-1}) dispersed in phosphate-buffered saline (PBS, pH 7.4). The PL of the NPs dissolved in the enhancer solution was found about 1×10^6 times stronger than that of the NPs with the same concentration dispersed in PBS (Table S1). To unravel the origin of the dissolution-enhanced PL, we compared the steady-state PL spectra and PL decay of the $NaEuF_4$ NPs before and after the dissolution. Both the steady-state PL profile and the PL decay of the NPs dissolved in the enhancer solution were significantly different from those of the NPs dispersed in PBS (Figures 3d,e). The PL excitation and emission spectra of the NPs in PBS exhibited characteristic and sharp spectral peaks with their dominant excitation and

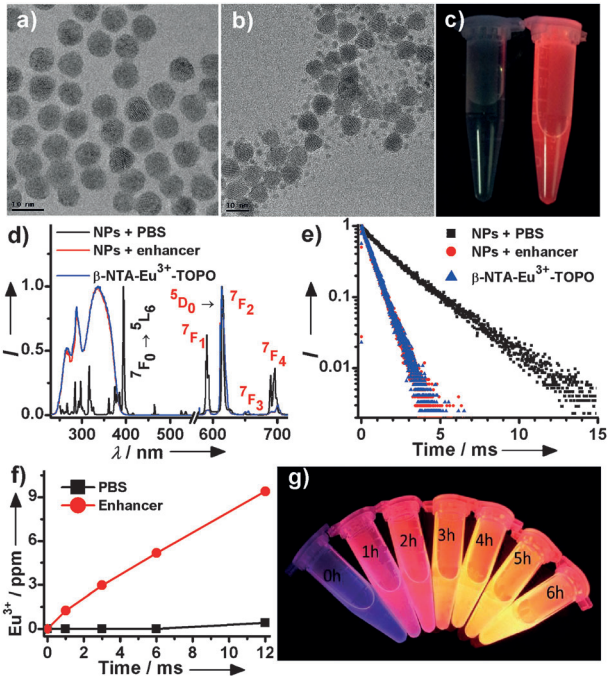

Figure 3. TEM images of a) ligand-free $NaEuF_4$ NPs and b) ligand-free $NaEuF_4$ NPs 1 minute after their addition to the enhancer solution (scale bars = 10 nm). c) Images showing the PL of ligand-free $NaEuF_4$ NPs in PBS (left) and the enhancer solution (right) under UV-lamp illumination at $\lambda = 300$ nm. d) Normalized PL excitation spectra (left) and emission spectra (right) of ligand-free $NaEuF_4$ NPs in PBS and the enhancer solution, and β-NTA–Eu^{3+}–TOPO ternary complex, respectively. e) The corresponding PL decays from $^5D_0$ by monitoring Eu^{3+} emission at $\lambda = 614$ nm. f) The concentration of Eu^{3+} ions in the dialysate of ligand-free $NaEuF_4$ NPs after 12 hours dialysis in the enhancer solution and PBS, respectively. g) Images of the dialysate for ligand-free $NaEuF_4$ NPs dialyzed in the enhancer solution under UV-lamp illumination at $\lambda = 300$ nm, retrieved at different time intervals (1–6 h).

emission bands peaking at $\lambda = 394$ and 614 nm, respectively. These bands arise from the intra-$4f^6$ transitions of the Eu^{3+} ions experiencing the crystal field in the $NaEuF_4$ lattice.[8a] In contrast, the NPs dissolved in the enhancer solution exhibited an unusual broad band at approximately $\lambda = 340$ nm in the excitation spectrum and distinct PL branching ratios for the $^5D_0 \rightarrow {}^7F_{1\text{-}4}$ transitions of Eu^{3+} in the emission spectrum. These bands were found to be identical to those of the β-NTA–Eu^{3+}–TOPO ternary complex formed by direct mixing of europium acetate with the enhancer solution (1 μg mL^{-1}). The PL lifetime of the NPs dissolved in the enhancer solution was determined consistently to be the same as that of the β-NTA–Eu^{3+}–TOPO complex (0.66 ms). This value is in good agreement with the PL lifetime of the β-NTA–Eu^{3+}–TOPO complex previously reported,[12] but significantly different from that of the original NPs in PBS (2.16 ms). These results indicate that the enhanced Eu^{3+} PL of the NPs dissolved in the enhancer solution originates from a β-NTA–Eu^{3+}–TOPO complex instead of $NaEuF_4$ NPs. The dissolution process of $NaEuF_4$ NPs is most likely as a result of the dynamic reaction between Eu^{3+} ions released from the NPs and β-NTA in the enhancer solution (Supporting Information).

The dissolution mechanism of $NaEuF_4$ NPs was further corroborated through dialysis experiments, where the aqueous solution of the NPs (1 mg mL^{-1}) was dialyzed in 1 L of the enhancer solution and PBS, respectively, by using a membrane with a molecular-weight cutoff of 3.5 kDa, which retains NPs but allows dissolved Eu^{3+} ions to pass through. Compositional analysis by inductively coupled plasma atomic emission spectroscopy (ICP-AES) revealed that the concentration of Eu^{3+} ions in the dialysate of the enhancer solution gradually increased with time, reaching a value of 9.4 ppm after 12 hours, whereas a negligible concentration of Eu^{3+} ions was found in the dialysate of PBS (Figure 3 f). Accordingly, the dialysate (1 mL) of the enhancer solution retrieved at different time intervals (1–6 hours) exhibited more intense red PL with increasing time under UV-lamp illumination (Figure 3 g). The increase in PL intensity indicates the higher concentration of β-NTA–Eu^{3+}–TOPO complex formed, which is consistent with the increased concentration of Eu^{3+} ions as evidenced by ICP-AES measurements.

To validate the feasibility of DELBA, we first evaluated the detection response and the linear range of the dissolution-enhanced PL. It was found that even for ligand-free $NaEuF_4$ NPs with a concentration as high as 10 μg mL^{-1}, its dissolution-enhanced PL signal reached a plateau within 1 minute upon addition of the enhancer solution (Figure 4 a), thus revealing the fast PL response of our nanoprobes. Moreover, the dissolution-enhanced PL signal increased gradually and exhibited a linear relationship with increasing concentration from 0 to 10 mg mL^{-1} (Figure 4 b), a finding of key importance for clinical bioassays. These results show the promise of $NaEuF_4$ nanoprobes in DELBA as an alternative to Ln^{3+} chelates in DELFIA.

Thanks to the exposed Eu^{3+} ions on the surface of the ligand-free $NaEuF_4$ NPs, biotin can be conjugated to the surface of NPs through the strong chelation of Eu^{3+} ions.[7b,10] The successful conjugation of biotin to the surface of the NPs was corroborated by the appearance of amide bands in the FTIR spectrum, as well as by changes in the decomposition temperature, weight losses, and ζ potentials for NPs before and after surface modification (Figures S3, S4, S6). By using an avidin/HABA reagent (HABA = 4'-hydroxyazobenzene-2-carboxylic acid),[13] the number of bound biotin molecules per NP was determined to be 4.5 ± 0.3 (Figure S7). These biotinylated NPs can indirectly capture the biotinylated biomolecules upon addition of avidin through biotin–avidin–biotin interactions.[14] By virtue of the specific recognition of the anti-CEA antibody with CEA, we employed biotinylated $NaEuF_4$ NPs as the nanoprobe in a sandwich-type DELBA for the detection of CEA. As illustrated in Figure 1 b, the capture anti-CEA antibody was first bound to the microplate well, and the biotinylated detection anti-CEA antibody (which was itself bound to CEA) was conjugated to the biotinylated nanoprobe through avidin. To avoid non-specific binding between the nanoprobes and the biotinylated antibody, we blocked the surface of the nanoprobes using bovine serum albumin (BSA) before labeling. CEA was quantified by measuring the dissolution-enhanced TRPL signal of the NPs upon addition of the enhancer solution on a multimodal microplate reader. For comparison, control

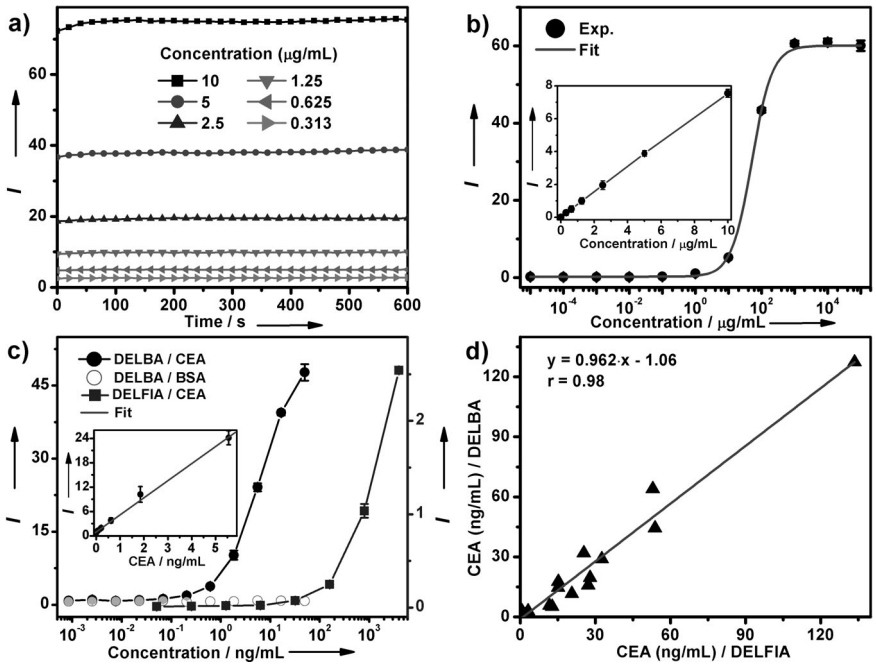

Figure 4. a) Time-dependent PL signal of ligand-free $NaEuF_4$ NPs at different concentrations upon addition of the enhancer solution (200 μL). b) Concentration-dependent dissolution-enhanced PL signal of $NaEuF_4$ NPs dissolved in the enhancer solution. Inset: the linear range of the dissolution-enhanced PL signal versus NP concentration (0–10 $\mu g\,mL^{-1}$). c) Calibration curves for the CEA assay using DELBA (based on $NaEuF_4$ NPs) and the commercial DELFIA kit (based on the Eu^{3+}–DTTA complex). Right-hand axis refers to DELFIA/CEA square data points. Gray circles indicate overlapped black and white circular data points. Inset: the linear range of the calibration curve for the CEA assay by DELBA. d) Correlation between DELBA and commercial DELFIA for the detection of CEA in 20 human serum samples. The axes indicate the CEA levels detected in DELBA (ordinate axis) and DELFIA (abscissa axis) experiments. b)–d) Each data point represents the mean (± standard deviation) of three independent experiments.

experiments by replacing CEA with BSA under otherwise identical conditions were also conducted. These control experiments show neglible TRPL signal, thus verifying the high specificity of DELBA. We also employed the commercial DELFIA kit for the CEA assay using the Eu^{3+}–DTTA complex as the molecular probe. For both DELBA and commercial DELFIA assays, the TRPL signal in the calibration curve for the CEA assay gradually increased with the CEA concentration (Figure 4c). In particular, the calibration curve in the DELBA assay for CEA exhibits an excellent linear dependence of PL intensity with concentration in the range of 0–10 $ng\,mL^{-1}$. The limit-of-detection (LOD), defined as the concentration that corresponds to three times the standard deviation above the signal measured in the control experiment, was determined to be approximately 0.1 $pg\,mL^{-1}$ (0.5 fM) in DELBA (Figure S8). This value represents an improvement of three orders of magnitude on that of the commercial DELFIA (90 $pg\,mL^{-1}$).[15]

Based on the above calibration curve, we carried out a series of experiments involving the in vitro detection of CEA in 20 human serum samples, of which 10 samples came from healthy humans and 10 samples from cancer patients. The CEA levels determined were compared with those independently measured using a commercial DELFIA kit (Table S2). The CEA levels derived from DELBA experiments are in good agreement with those obtained from DELFIA. The correlation coefficient between both methods was determined to be 0.98 ± 0.02 (Figure 4d). Furthermore, we evaluated the analytical accuracy and precision of DELBA through the determination of the CEA level, coefficient of variation (CV), and the recovery of two human serum samples upon addition of human CEA standard solutions with different concentrations. The CVs of all assays are below 8% and the analytical recoveries are in the range of 95–105% (Table S3), both of which are within the acceptance criteria (CVs $\leq 15\%$; recoveries in the range of 90–110%) set for bioanalytical method validation.[16] These results show unambiguously that the DELBA procedure established herein has high sensitivity and reliability, revealing its great potential as an ultrasensitive bioassay platform in clinical applications.

In addition to employing the $NaEuF_4$ nanoprobe and the β-NTA enhancer solution, we also explored the DELBA system using other Ln^{3+}-based NPs or enhancer solutions. For example, intense red PL can be detected upon addition of ligand-free $NaSmF_4$ NPs to the β-NTA-containing enhancer solution (Figure S9). This PL was revealed to originate from a β-NTA–Sm^{3+}–TOPO complex (Figure S10). By utilizing the dissolution-enhanced PL of $NaSmF_4$ NPs, we successfully achieved the detection of CEA with an LOD of 1.2 $pg\,mL^{-1}$ (6.0 fM) (Figure S11). Similarly, we extended the DELBA system by employing ligand-free $NaTbF_4$ NPs and an enhancer solution containing 5-fluorosalicylic acid (5-FSA; data not shown). These results fully support the generality of DELBA with diverse combinations of Ln^{3+} NPs and enhancer solutions.

In summary, we have developed the ultrasensitive luminescent bioassay DELBA which is based on the dissolution-enhanced PL of inorganic Ln^{3+} NPs. As a result of the highly concentrated Ln^{3+} ions in a single NP, a much higher labeling ratio of Ln^{3+} ions per biomolecule can be achieved. Upon dissolution of the NPs by the enhancer solution, a myriad of Ln^{3+} ions can be released and transformed into highly luminescent Ln^{3+} micelles, which amplifies the TRPL signal and thus improves the detection sensitivity compared to that of the commercial DELFIA. In particular, by employing sub-10 nm $NaEuF_4$ NPs along with the β-NTA-containing enhancer solution, an unprecedented amplification (10^6 times) of the PL signal of the dissolved NPs has been achieved. By using such intense dissolution-enhanced PL, we have achieved the detection of CEA in human serum samples with an LOD as low as 0.5 fM, which is an improvement of

approximately 3 orders of magnitude on that of commercial DELFIA. These findings offer new opportunities towards advances in clinical bioassays, thereby opening up new avenues for the exploration of inorganic lanthanide NPs in versatile bioapplications, such as in the diagnosis of early-stage cancers.

Received: June 6, 2014
Revised: July 1, 2014
Published online: August 11, 2014

Keywords: bioassays · lanthanides · luminescence · tumor markers · nanoparticles

[1] a) A. Sassolas, B. D. Leca-Bouvier, L. J. Blum, *Chem. Rev.* **2008**, *108*, 109 – 139; b) D. T. Tu, W. Zheng, Y. S. Liu, H. M. Zhu, X. Y. Chen, *Coord. Chem. Rev.* **2014**, *273 – 274*, 13 – 29.

[2] a) A. E. Herr, A. V. Hatch, D. J. Throckmorton, H. M. Tran, J. S. Brennan, W. V. Giannobile, A. K. Singh, *Proc. Natl. Acad. Sci. USA* **2007**, *104*, 5268 – 5273; b) J. V. Jokerst, A. Raamanathan, N. Christodoulides, P. N. Floriano, A. A. Pollard, G. W. Simmons, J. Wong, C. Gage, W. B. Furmaga, S. W. Redding, J. T. McDevitt, *Biosens. Bioelectron.* **2009**, *24*, 3622 – 3629.

[3] a) S. M. Borisov, O. S. Wolfbeis, *Chem. Rev.* **2008**, *108*, 423 – 461; b) J.-C. G. Bünzli, *Chem. Rev.* **2010**, *110*, 2729 – 2755; c) M. Seydack, *Biosens. Bioelectron.* **2005**, *20*, 2454 – 2469; d) X. D. Wang, O. S. Wolfbeis, R. J. Meier, *Chem. Soc. Rev.* **2013**, *42*, 7834 – 7869.

[4] a) N. J. Cowans, A. Stamatopoulou, J. Hellström, M.-M. Mäkelä, K. Spencer, *Prenatal Diagn.* **2010**, *30*, 127 – 132; b) I. Hemmilä, S. Dakubu, V.-M. Mukkala, H. Siitari, T. Lövgren, *Anal. Biochem.* **1984**, *137*, 335 – 343; c) H. Siitari, I. Hemmila, E. Soini, T. Lovgren, V. Koistinen, *Nature* **1983**, *301*, 258 – 260.

[5] E. P. Diamandis, *Clin. Biochem.* **1988**, *21*, 139 – 150.

[6] a) J.-C. G. Bünzli, C. Piguet, *Chem. Soc. Rev.* **2005**, *34*, 1048 – 1077; b) Y. Chen, Y. Chi, H. Wen, Z. Lu, *Anal. Chem.* **2006**, *79*, 960 – 965.

[7] a) R. R. Deng, X. J. Xie, M. Vendrell, Y. T. Chang, X. G. Liu, *J. Am. Chem. Soc.* **2011**, *133*, 20168 – 20171; b) P. Huang, W. Zheng, S. Y. Zhou, D. T. Tu, Z. Chen, H. M. Zhu, R. F. Li, E. Ma, M. D. Huang, X. Y. Chen, *Angew. Chem.* **2014**, *126*, 1276 – 1281; *Angew. Chem. Int. Ed.* **2014**, *53*, 1252 – 1257; c) Q. Liu, W. Feng, T. S. Yang, T. Yi, F. Y. Li, *Nat. Protoc.* **2013**, *8*, 2033 – 2044; d) J. Shen, L. D. Sun, J. D. Zhu, L. H. Wei, H. F. Sun, C. H. Yan, *Adv. Funct. Mater.* **2010**, *20*, 3708 – 3714; e) L. Y. Wang, R. X. Yan, Z. Y. Huo, L. Wang, J. H. Zeng, J. Bao, X. Wang, Q. Peng, Y. D. Li, *Angew. Chem.* **2005**, *117*, 6208 – 6211; *Angew. Chem. Int. Ed.* **2005**, *44*, 6054 – 6057; f) W. Zheng, S. Y. Zhou, Z. Chen, P. Hu, Y. S. Liu, D. T. Tu, H. M. Zhu, R. F. Li, M. D. Huang, X. Y. Chen, *Angew. Chem.* **2013**, *125*, 6803 – 6808; *Angew. Chem. Int. Ed.* **2013**, *52*, 6671 – 6676.

[8] a) X. Y. Chen, Y. S. Liu, D. T. Tu, *Lanthanide-doped Luminescent Nanomaterials: From Fundamentals to Bioapplications*, Springer, Berlin, **2014**; b) Y. S. Liu, D. T. Tu, H. M. Zhu, X. Y. Chen, *Chem. Soc. Rev.* **2013**, *42*, 6924 – 6958.

[9] Z. Q. Li, Y. Zhang, *Nanotechnology* **2008**, *19*, 345606.

[10] G. A. Ozin, N. Bogdan, F. Vetrone, J. A. Capobianco, *Nano Lett.* **2011**, *11*, 835 – 840.

[11] Y. J. Zhang, F. Zheng, T. L. Yang, W. Zhou, Y. Liu, N. Man, L. Zhang, N. Jin, Q. Q. Dou, Y. Zhang, Z. Q. Li, L. P. Wen, *Nat. Mater.* **2012**, *11*, 817 – 826.

[12] K. A. Gschneidner, J.-C. G. Bünzli, V. K. Pecharsky, *Handbook on the Physics and Chemistry of Rare Earths*, *Vol. 37*, Springer-Verlag Press, Berlin, **2007**.

[13] X. J. Wang, L. Liu, Y. Luo, H. Y. Zhao, *Langmuir* **2009**, *25*, 744 – 750.

[14] E. R. Goldman, E. D. Balighian, H. Mattoussi, M. K. Kuno, J. M. Mauro, P. T. Tran, G. P. Anderson, *J. Am. Chem. Soc.* **2002**, *124*, 6378 – 6382.

[15] J. Yuan, G. Wang, K. Majima, K. Matsumoto, *Anal. Chem.* **2001**, *73*, 1869 – 1876.

[16] V. P. Shah, K. K. Midha, J. W. Findlay, H. M. Hill, J. D. Hulse, I. J. McGilveray, G. McKay, K. J. Miller, R. N. Patnaik, M. L. Powell, A. Tonelli, C. T. Viswanathan, A. Yacobi, *Pharm. Res.* **2000**, *17*, 1551 – 1557.

